An Integrated Model for Performance Optimization of Aerospace Bearings Considering High-Speed Rotations and Temperature Variations

Aydın Gündüz*
Technical Specialist
Power Transmission Systems Design

Zihni Burçay Sarıbay
Power Transmission Systems Design Manager

Sinan Yılmaz
Design Engineer
Power Transmission Systems Design

Turkish Aerospace Industries, Ankara, Turkey

In this work, a comprehensive analytical model is established to study the performance of the bearings of a helicopter high-speed-input gear shaft. The high-speed shaft, rotating above 15,000 rpm, transmits power to the second stage through a bevel gear that is straddle mounted by a duplex ball bearing and a cylindrical roller bearing. The effects of centrifugal forces, the change of bearing internal clearances due to interference fits, and uneven thermal expansions are studied in the outlined approach. Then the influence of temperature elevations (that may arise due to inadequate cooling) on the performance of high-speed bearings is explored by employing the proposed model. This study emphasizes that bearing internal clearances are very critical in assessing the performance of the high-speed system and optimal manufactured bearing clearances are greatly dependent on the operating conditions. Thus, a bearing internal clearance optimization study is carried out considering a broad range of operating temperatures. This optimization study provides "operation condition maps" for high-speed bearings and guides the designer for the optimal selections of bearing clearances by considering different conditions.

Nomenclature

A_o	unloaded distance between inner and outer curvature centers, mm
D	rolling element diameter, mm
D_f	fit diameter, mm
D_o	outer fit diameter, mm
d_h	housing outer diameter, mm
d_i, d_o	raceway groove diameters, mm
d_m	pitch diameter of the bearing, mm
d_s	shaft bore diameter, mm
d_1	outer body OD of the fitting body 1, mm
d_2	inner body ID of the fitting body 2, mm
E	elastic modulus, Pa
F	bearing load vector
F_c	centrifugal force, N
I	interference between fitting parts, μm
K_n	Hertzian stiffness constant. N/mmn
L_{10}	bearing L10 life, h
l	roller length, mm
n	load-deflection exponent (1.5 for ball; 1.11 for rollers)
n_m	rotational speed of the high-speed shaft, rpm
P_d	radial clearance, μm
p	contact pressure between fitting parts, Pa
q	bearing deflection vector
R	pitch radius, mm
T	temperature, °C
Z	number of rolling elements
α_o	unloaded contact angle, deg
Γ	coefficient of linear thermal expansion, m/m·°C
δ_r	radial deflection of the rolling element, mm
δ_z	axial deflection of the rolling element, mm
υ	Poisson's ratio
ψ	azimuth angle, deg

Subscripts

a	ambient
e	rolling element
h	housing
i	inner ring
j	rolling element (ball or roller) index
k	bearing index ($k = 1,2,3$)
o	outer ring
r	radial magnitude
s	shaft
x, y	radial directions
z	axial

*Corresponding author; e-mail: aydin.gunduz@tai.com.tr.
Presented at the AHS 71st Annual Forum, Virginia Beach, VA, May 5–7, 2015.
Manuscript received May 2015; accepted August 2017.

DOI: 10.4050/JAHS.63.012004

1 fitting body 1 (hole)
2 fitting body 2 (shaft)

Introduction

The design of high-speed bearing systems for aerospace applications is a challenging problem that requires reconciling many demanding, even conflicting design criteria. As being the most critical components of the high-speed stage, rolling element bearings face several challenges during their operation, some of which are listed as follows:

1) At high speeds, centrifugal effects become critical (particularly for all-steel bearings) generating considerable loads and increased contact stresses at the bearing outer raceway.

2) Centrifugal effects force the rolling elements to the outer race, thus, outer contact angle shrinks and inner contact angle expands for an angular contact bearing. This disrupts the colinearity of the contact line and causes instability and increased vibration.

3) Increased skidding and wear of rollers.

4) Excessive friction and heat generation at the raceways (especially for all-steel bearings).

Owing to the large amount of heat generation at the raceways and being in the vicinity of powerful heat generators (i.e., engines), high-speed shaft and bearings may reach undesired operating temperatures if the cooling conditions are not ideal. Such high-temperature levels affect bearing fits, internal clearances, and oil film thickness. Consequently, significant elevations in bearing contact stresses, increased wear, increased risk of crack initiation and fracture, and dramatic reductions in bearing life may be expected. To overcome such complex and interdependent challenges, high-speed bearings of helicopter transmission systems must be mindfully designed.

The strength and durability of high-speed bearings in helicopter transmission systems has been an area of interest for helicopter companies and researchers in the field (Refs. 1–5). These studies, however, are mostly concerned with the design of high-speed bearings and do not focus on the effects of temperature elevations and its consequences of high-speed bearing performance. In the field of machining and manufacturing, numerous thermomechanical models have been proposed (Refs. 6–8) to investigate the thermal performance of high-speed bearings, though it is usually difficult to generalize these methods for other applications without precise knowledge of thermal characteristics of the system.

This study outlines a comprehensive analytical approach for a high-speed bearing system that takes the effects of centrifugal forces and high operating temperatures into consideration. By utilizing the outlined mathematical model, the influence of temperature increases within the system (due to poor cooling or any other reasons) on the performance of high-speed bearings may be observed. This examination will point out that the optimal clearance of high-speed bearings is greatly dependent on the operating conditions. Thus, this work also introduces an optimization study of the bearing internal clearance of high-speed bearings, showing that the manufactured internal clearance of the bearings should be carefully selected considering potential operating conditions of the system.

Scope, Assumptions, and Objectives

A two-dimensional (2D) schematic of the high-speed pinion-shaft investigated in this study is presented in Fig. 1. The high-speed shaft rotates above 15,000 rpm and transmits power to the second stage through a bevel gear that is straddle mounted by a duplex ball bearing arrangement and a cylindrical roller bearing (CRB), which is integral with the shaft. The duplex arrangement consists of an angular contact (ACBB), and a three-point contact (3 PCB) ball bearing; so that the unit provides sufficient rigidity against moderate-heavy axial gear loads, yet it can support thrust loads in the opposite direction with minimal weight addition to the system. The high-speed bearings are made of VIMVAR M50 steel. Housing is made of cast aluminum alloy and being cooled by external airflow. Bearings are mounted on steel liners that are tightly fitted into the housing. It is assumed up to a maximum 1200 HP is transmitted through the shaft, and bearing performances are evaluated using a representative continuous power load case. The bearings are lubricated and cooled by an ester-based, high-viscosity index, synthetic oil.

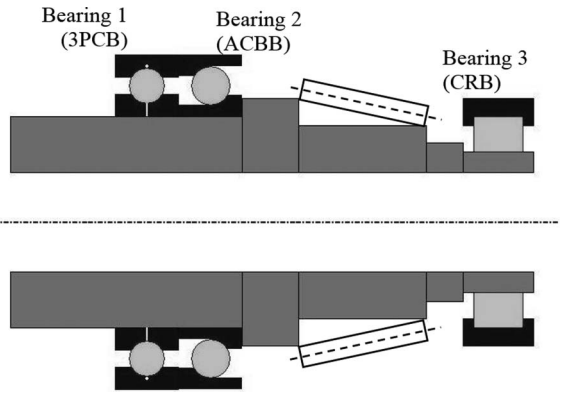

Fig. 1. 2D illustration of a generic helicopter high-speed shaft supported by a duplex tandem ball bearing and a CRB.

In this study, the effects of transient loading and torque reversals are neglected and steady-state loading is assumed. Under constant thrust load, 3 PCB (bearing 1) functions similar to ACBB and shares the thrust load with bearing 2; thus, the unit is treated as a duplex tandem ball bearing configuration. Contact angle and internal details of these two bearings are identical. Owing to uneven thermal expansion of the parts, the bearings acquire thermal preloads during the operation; these effects are included in the model. These thermal preloads may cause excessive friction and unstable temperature rise. If the cooling is inadequate, the contacting metal parts can be a subject of "temperature rise–uneven thermal growth of metal parts–increased friction–further temperature increase" loop, which could have catastrophic results. This is a primary reason bearing operating clearance is very critical, particularly when extreme conditions such as no oil running are considered.

This study assumes that there is always some liquid lubricant exists between the contacting metal parts, either in the form of thin film, partial or full film elastohydrodynamic lubrication (EHL). The effects of insufficient or ineffective lubrication are expressed in terms of temperature elevations; as well as included in "lubrication factor" (a_3) for bearing life calculations. The analytical investigation of "no oil" condition is beyond the scope of this study, as dry running condition requires special thermal analyses, and bearing life calculations are not valid under this condition.

Radial thermal expansion of the shaft, bearing rings, rolling elements, and the housing are incorporated in the analytical model. However, the axial thermal expansion of the shaft is neglected as the axial load-carrying (tandem ball) bearings are located side by side. The cylindrical roller located at the end allows free axial elongation of the shaft and compensates any thermal stresses.

This study does not aim to predict the operating temperatures of the rotating parts; because even the well-established and sophisticated analytical or finite element thermomechanical models may yield inaccurate results without precise knowledge of the thermal characteristics of the system, which is usually obtained by field experience or testing. In this study, a temperature rise model representing a severe level of insufficient cooling is utilized based on earlier experience and assumptions.

According to this model:

1) The normal (initial) temperature difference between the inner and outer races of high-speed bearings is 15°C (where $T_i = 90$°C; $T_o = 75$°C). This is a typical temperature gradient for the high-speed-input stage where the housing is cooled by external airflow. The temperature of the oil and rolling elements is assumed 85°C at this condition.

2) The outer ring of the bearings has the same operating temperature with the housing; similarly, bearing inner rings have the same operating temperatures with the high-speed shaft.

3) The temperature rise of the system occurs in such a way that for every 15°C increase of the shaft (and inner rings), the temperature of the housing (and outer rings) rises by 9°C (i.e., $5\Delta T_{\text{out}} = 3\Delta T_{\text{in}}$). The main reasons for this differential are the large heat capacity difference between the housing and the shaft (i.e., the heat capacity of the hollow shaft is much smaller than the heat capacity of the housing so that the temperature of the shaft increases faster), and the fact that housing is being cooled by an external airflow.

4) For every 15°C increase of the shaft, the temperature of the oil and rolling elements rises by 14°C. As the generated heat flows radially outwards, oil and the rolling elements are expected to have an intermediate temperature between inner and outer rings. However, as they are in contact with points of heat generation, the temperature increase of the oil and rolling elements is only slightly less than that of the inner rings.

5) The ambient temperature (T_a) at which the parts are mounted is accepted as 20°C.

Previous research (Ref. 6) has shown that the "softening" effect of very high speeds on bearing stiffness is usually negligible compared to bearing stiffness increase due to uneven thermal expansion of the bearing parts. Therefore, it is assumed that high speeds do not affect the stiffness of the bearing alone. System and rotor dynamics aspects of the problem and vibration characteristics of the high-speed system are beyond the scope of this study. The specific objectives of this study are listed as follows:

1) Develop a comprehensive analytical model for the high-speed shaft-bearing system by taking high-speed effects, temperature variations, mounting and thermal expansion effects, and bearing internal clearance reductions into consideration.

2) Utilize the developed model to investigate the effects of temperature elevations on the performance of high-speed bearings of a concept helicopter gearbox.

3) Using the developed model, carry out a clearance optimization study for the high-speed bearings to determine the ideal manufactured clearances considering different operating conditions.

Analytical Model

High-speed shaft and bearings

A schematic of the analytical model of the high-speed system is shown in Fig. 2. In this model, the high-speed shaft is modeled as a finite element Timoshenko beam, and the bearings are represented as five-dimensional nonlinear stiffness elements with cross-coupling terms but no torsional stiffness. The gear mesh forces are applied as a point load on the shaft to the center of gear face width, which consist of radial, axial, and moment loads.

Multidimensional, nonlinear load-deflection characteristics of rolling bearings define the boundary conditions for the shaft (and hence, nonlinear spring terms for the bearings). If $\boldsymbol{F}^k = \{F_x^k\ F_y^k\ F_z^k\ M_x^k\ M_y^k\}$ and $\boldsymbol{q}^k = \{\delta_x^k\ \delta_y^k\ \delta_z^k\ \beta_x^k\ \beta_y^k\}$ respectively represent the five-dimensional load and displacement vectors of the kth rolling element bearing ($k = 1, 2, 3$), the relationship between two can be established by considering the elastic deformation between each rolling element and bearing races; and this

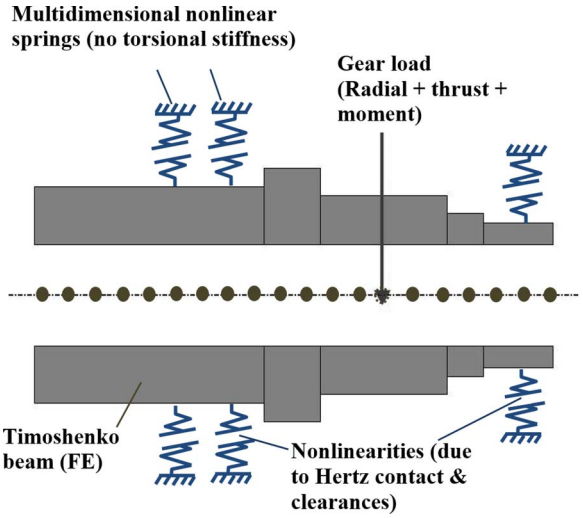

Fig. 2. Schematic illustrating the mathematical model of the high-speed shaft system presented in Fig. 1.

relationship is defined by Hertzian contact theory (Refs. 9–11). For ball bearings, this can be written in the expanded form as shown in Eq. (1). Here, δ_{rj}^k and δ_{zj}^k denote the radial and axial deflections of the jth rolling element of the kth bearing and can be expressed in terms of the elements of $\boldsymbol{q}^k$ as given in Eqs. (2) and (3) (refer to the Nomenclature for all other symbols):

$$F^k = \begin{Bmatrix} F_x^k \\ F_y^k \\ F_z^k \\ M_x^k \\ M_y^k \end{Bmatrix} = K_n \sum_{j=1}^{Z^k} \frac{\left\{\left[\left(A_o^k \sin\left(\alpha_o^k\right) + \delta_{zj}^k\right)^2 + \left(A_o^k \cos\left(\alpha_o^k\right) + \delta_{rj}^k\right)^2\right]^{1/2} - A_o^k\right\}^n}{\left[\left(A_o^k \sin\left(\alpha_o^k\right) + \delta_{zj}^k\right)^2 + \left(A_o^k \cos\left(\alpha_o^k\right) + \delta_{rj}^k\right)^2\right]^{1/2}} \times \begin{Bmatrix} \left(A_o^k \cos\left(\alpha_o^k\right) + \delta_{rj}^k\right) \cos\left(\psi_j^k\right) \\ \left(A_o^k \cos\left(\alpha_o^k\right) + \delta_{rj}^k\right) \sin\left(\psi_j^k\right) \\ \left(A_o^k \sin\left(\alpha_o^k\right) + \delta_{zj}^k\right) \\ R^k \left(A_o^k \sin\left(\alpha_o^k\right) + \delta_{zj}^k\right) \sin\left(\psi_j^k\right) \\ -R^k \left(A_o^k \sin\left(\alpha_o^k\right) + \delta_{zj}^k\right) \cos\left(\psi_j^k\right) \end{Bmatrix}. \quad (1)$$

$$\delta_{rj}^k = \delta_x^k \cos\left(\psi_j^k\right) + \delta_y^k \sin\left(\psi_j^k\right) - P_d^k \quad (2)$$

$$\delta_{zj}^k = \delta_z^k + R^k \left[\beta_x^k \sin\left(\psi_j^k\right) - \beta_y^k \cos\left(\psi_j^k\right)\right] \quad (3)$$

Similarly, the load-deflection relationship for roller bearings can be written in the following form:

$$F^k = \begin{Bmatrix} F_x^k \\ F_y^k \\ F_z^k \\ M_x^k \\ M_y^k \end{Bmatrix} = K_n \sum_{j=1}^{Z^k} \left[\delta_{rj}^k \cos\left(\alpha_o^k\right) \delta_{zj}^k \sin\left(\alpha_o^k\right)\right]^n \times \begin{Bmatrix} \cos\left(\alpha_o^k\right) \cos\left(\psi_j^k\right) \\ \cos\left(\alpha_o^k\right) \sin\left(\psi_j^k\right) \\ \sin\left(\alpha_o^k\right) \\ R^k \sin\left(\alpha_o^k\right) \sin\left(\psi_j^k\right) \\ -R^k \sin\left(\alpha_o^k\right) \cos\left(\psi_j^k\right) \end{Bmatrix} \quad (4)$$

Equations (2) and (3) may also be used for roller bearings to express δ_{rj}^k and δ_{zj}^k. The nonlinear iterative problem of the Timoshenko beam with such boundary conditions is solved by a "trust-region-reflective" optimization algorithm as described in Ref. 12.

Fitting and thermal expansion effects

As relatively heavier loads are involved in the application, both inner (if exist) and outer rings of high-speed bearings are mounted with a certain interference to reduce resilience, vibrations, and rattle. The amount of interference between fitting parts before any thermal effects is given by Eq. (5) (Ref. 13):

$$I = pD_f \left\{ \frac{1}{E_1} \left[\frac{(d_1/D_f)^2 + 1}{(d_1/D_f)^2 - 1} + \upsilon_1 \right] + \frac{1}{E_2} \left[\frac{(D_f/d_2)^2 + 1}{(D_f/d_2)^2 - 1} + \upsilon_2 \right] \right\} \tag{5}$$

A variation in the thermal expansion coefficients between the fitting parts can affect the fit during the operation. As the coefficient of linear thermal expansion for aluminum is greatly higher than that of steel (23 vs. 12 μm/m $\cdot^\circ$ C), there is a risk of loss of the desired fit at the outer ring housing interface at high operating temperatures. This is especially a significant problem for the ringless CRB, which could result in looseness and excessive shaft deflections. Using a heavy interference fit for the outer ring is not a desired solution because it causes negative bearing internal clearance at the mounting temperature. An effective solution to overcome this problem is the utilization of steel liners between the housing and outer rings as illustrated in Fig. 3. In this case, a heavy interference fit is ensured between the liner and housing to prevent the separation even at the highest housing temperatures. Table 1 shows the interfaces that exist in the high-speed system along with their tightness level.

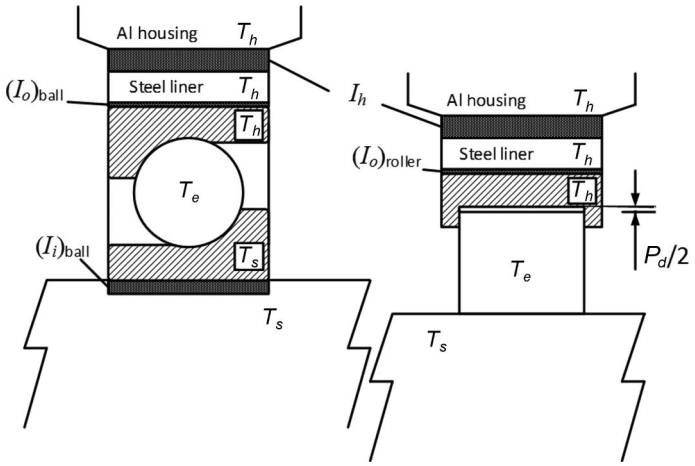

Fig. 3. Schematic illustrating the fits of high-speed bearings along with their operating temperatures.

Table 1. Interference fit levels of the high-speed bearings

Interface	Bearing Type	Interference Tightness
Shaft–inner ring (I_i)	Duplex ball	Medium
	Roller	–
Outer ring–liner (I_o)	Duplex ball	Light
	Roller	Light
Liner–housing (I_h)	Both	Heavy

To determine the minimum amount of interference at the liner-housing interface, Eq. (6) may be used. To maintain the interference $I_h - \Delta I_h > 0$ must be satisfied:

$$\Delta I_h = (\Gamma_h - \Gamma_o) D_o (T_o - T_a) \tag{6}$$

Manufactured, mounted, and operating clearance

Manufactured clearance of rolling element bearings is affected by shaft and housing mounting and uneven thermal expansion of the bearing parts. The change of bearing internal clearances due to inner (Δ_s) and outer fits (Δ_h) is calculated according to Eqs. (7) and (8) (Ref. 13):

$$\Delta_s = \frac{-2I_i(d_i/D_i)}{[(D_i/d_i)^2 - 1]\left\{\left[\frac{(d_i/D_i)^2+1}{(d_i/D_i)^2-1} + \upsilon_b\right] + \frac{E_b}{E_s}\left[\frac{(D_i/d_s)^2+1}{(D_i/d_s)^2-1} + \upsilon_s\right]\right\}} \tag{7}$$

$$\Delta_h = \frac{-2I_o(D_o/d_o)}{[(D_o/d_o)^2 - 1]\left\{\left[\frac{(D_o/d_o)^2+1}{(D_o/d_o)^2-1} + \upsilon_b\right] + \frac{E_b}{E_h}\left[\frac{(d_h/D_o)^2+1}{(d_h/D_o)^2-1} + \upsilon_h\right]\right\}} \tag{8}$$

Symbols used here are consistent with Eq. (5), and negative results correspond to the reduction in bearing clearance. The calculated bearing clearance before any consideration of the thermal effects is the "mounted clearance." The change of bearing internal clearance due to thermal expansion effects are then calculated as

$$\Delta_T = \Gamma_b \left[d_o (T_o - T_a) - d_i (T_i - T_a) - 2D (T_e - T_a) \right] \tag{9}$$

Here the terms inside the brackets correspond to clearance change due to radial expansion of outer ring, inner ring, and rolling elements. As seen from Eq. (9), the expansion of outer ring extends the bearing clearance, whereas expansion of inner ring and rolling elements tend to diminish it. If operating temperatures of these three parts are equal (i.e., $T_o = T_i = T_e$), the net change of the internal clearance is zero regardless of T_a since $d_o \cong d_i + 2D$. However, typically $T_i > T_e > T_o$; thus, Δ_T is negative, which corresponds to a reduction in bearing internal clearance. When Δ_T exceeds the mounted clearance, internal clearance of the bearing is completely diminished and the bearing starts to acquire thermal preloads. The net change in diametral clearance as a result of interference mounting and thermal effects is expressed with

$$\Delta \mathrm{P}_d = \Delta_T + \Delta_h + \Delta_s \tag{10}$$

It should be noted that, in addition to the nature of Hertzian contact, bearing clearances are the primary source of nonlinear behavior of rolling bearings and have a key role on the load share among the bearings, as well as on the internal load distribution of each individual bearing. Therefore, maximum care should be taken during design to ensure an appropriate operating clearance. To minimize bearing stresses and attain optimal bearing lives, ideal load distributions among rolling elements must be achieved and preserved. This is accomplished by optimization of bearing internal clearances, which is discussed more in detail in the Clearance Optimization Study section of this article.

Influence of centrifugal effects

In high-speed bearing systems, centrifugal effects are another major factor influencing the internal load distribution of the bearings. At high-speeds, rolling elements apply considerable centrifugal loads (proportional to the square of the rotational speed) and cause increased contact stresses on the outer race. In addition, as rolling elements of an angular contact ball bearing are forced toward the outer ring, bearing contact

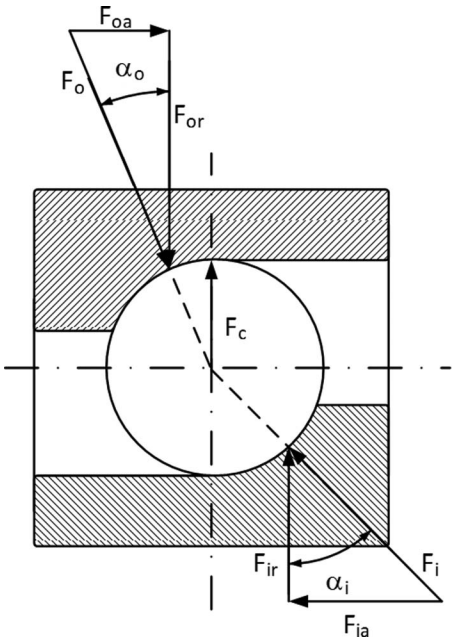

Fig. 4. Angular contact bearing under the effect of centrifugal forces.

line loses its collinearity, and the outer contact angle (α_o) of the bearing shrinks and inner contact angle (α_i) expands as shown in Fig. 4.

Using the conditions of equilibrium and assuming bearing rings are not flexible, F_o and α_o, can be determined as follows (Ref. 14):

$$\alpha_o = \cot^{-1}\left(\cot(\alpha_i) + \frac{F_c}{F_{ia}}\right) \tag{11}$$

$$F_o = \left[1 + \left(\cot(\alpha_i) + \frac{F_c}{F_{ia}}\right)^2\right]^{1/2} F_{ia} \tag{12}$$

where

$$F_c = \frac{\pi^3 \rho}{10{,}800g} D^3 n_m^2 d_m \tag{13}$$

defines the centrifugal load. If the expansion of the inner contact angle (or the shrinkage of the outer contact angle) is excessive, the risk of ellipse (contact area) truncation arises. To avoid this risk, the initial contact angle, shoulder height, and the conformity of the ball bearings should be properly selected for high-speed systems.

For the CRB, the centrifugal forces generated by rollers on the bearing outer race are determined as

$$F_c = 3.39 \times 10^{-11} D^2 n_m^2 d_m l \tag{14}$$

Analysis and Discussion

The temperature elevation model of the high-speed system is presented in Fig. 5. Slopes of the curves are in consistence with the temperature rise model explained earlier (all results will be presented against the housing temperature after this point)

Figures 6(a) and 6(b) illustrate the variation of bearing radial clearances for the ball and roller bearings, respectively. The contact angle of the angular contact ball bearings depends on the radial clearance, and the operating contact angle (before any centrifugal effects) decreases with reducing radial clearance. CRBs, however, are manufactured with a certain amount of radial clearance (termed as "manufactured clearance"). In this case, the manufactured clearance is accepted as 20 μm (this is

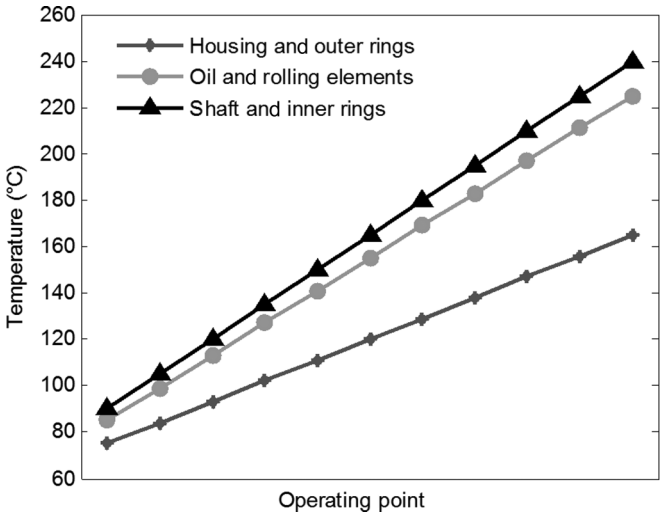

Fig. 5. Temperature elevation model of the high-speed system.

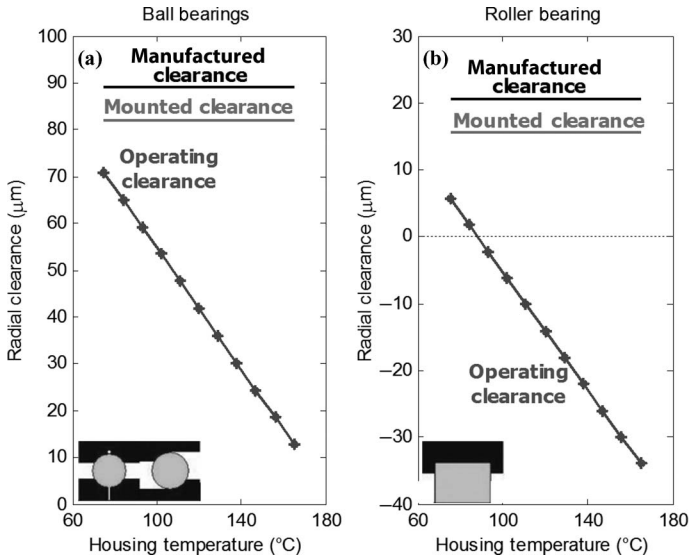

Fig. 6. Variation of bearing radial clearances with respect to operating temperature.

close to C2 clearance class, which is 17.5 μm for a bearing of this size). This relatively small clearance amount is selected as it provides a favorable internal load distribution within the roller bearing by loading higher number of rollers so that the maximum contact stresses on the bearing rings are reduced under ideal conditions. Owing to interference fitting, this clearance is reduced by about 5 μm (to 15 μm); this is the "mounted clearance" of the CRB at 20°C. The internal clearance is further reduced during operation due to uneven thermal expansion of the bearing parts. The variation of the operating clearance with temperature is shown (with marked curve) in Fig. 6(b). As seen, when $T_h \approx 85$°C, the radial clearance of the CRB is completely closed and the bearing starts to acquire thermal preload in the radial direction.

Figure 7 demonstrates the rise of the maximum contact stress of all three bearings with increasing operating temperature. It is observed that the contact stress of bearing 1 (3PCB) remains relatively flat and the change is relatively insignificant compared to other two bearings. The peak contact stress of bearing 2 (ACBB) shows a steeper elevation

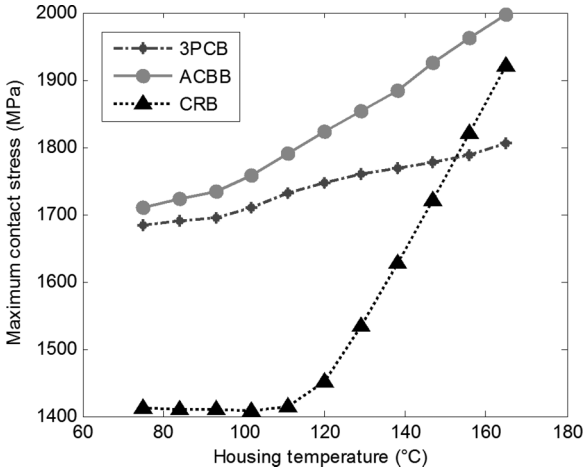

Fig. 7. Rise of the maximum contact stresses on the bearing raceways with increasing operating temperature.

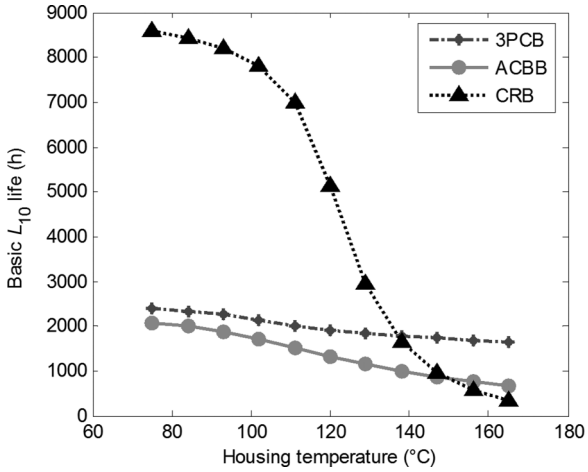

Fig. 8. Reduction in basic L_{10} life of system bearings with increasing operating temperature.

especially above 100°C and approaches 2000 MPa at higher temperatures. Bearing 3, on the other hand, shows a different behavior, where the contact stresses remain fairly flat up to 110°C. At this temperature, the operating clearance of the bearing is about $-5\,\mu$m; showing that the CRB is able to tolerate slight amount of negative operating clearance. Above 110°C, however, the maximum contact stress on the raceways rise extremely rapidly (from 1400 MPa to above 1900 MPa), which confirm that a negative operating clearance for the CRB is absolutely not tolerable unless it is very small. Another observation here is a negative operating clearance for the CRB influences the performance of the high-speed system (both on individual bearing and system level) significantly more than the thermal effects induced on the angular contact ball bearings. This is because of the nature of these two different types of bearings. In case of uneven thermal expansion of bearing parts, angular contact ball bearings in tandem configuration have reduced radial clearance (and contact angle) to alleviate the high contact stresses; whereas a CRB has to operate under negative operating clearance if the temperature differential between expanding parts is significant. The results presented here are for a continuous power load case; under extreme loading conditions, the contact stresses on the raceways could look much more dramatic with such high thermal preloads applied on the bearings.

Basic life calculations of the bearings, as shown in Fig. 8, are consistent with the contact stress results. Here, basic L_{10} lives of the bearings are calculated according to ISO/TS 16281 (Ref. 15), considering the effects of internal load distribution, misalignments, bearing tilting moments, and internal clearances. Dramatic reduction in bearing life for the CRB above 110°C is due to rapid increase of the contact stresses.

The increase in the operating temperature does not only influence the bearing performance by diminishing internal clearances, but it also considerably affects the lubrication characteristics because of reduced oil viscosity. Modified L_{10} lives of the bearings are calculated incorporating the life adjustment factors:

$$L_{10m} = a_1\, a_2 a_3 L_{10} \tag{15}$$

Here, the reliability factor (a_1) is "1" (for L_{10} life), the material and processing factor (a_2) is selected according to Refs. 16 and 17, and VIMVAR M50 steel provides a significant boost to bearing life. The lubrication factor (a_3) is strictly dependent on the oil film thickness parameter (Λ), defined as the ratio of the minimum film thickness to average surface roughness of the contacting metal parts. Common EHL theory (as explained in Ref. 14) is utilized to calculate the minimum film thickness. The variation of Λ and a_3 are shown in Figs. 9(a) and 9(b). As seen, the lubrication factor drops sharply up to $T_h = 120$°C due to reducing film thickness. Beyond this temperature, a_3 remains relatively flat at 0.15. At this point, lubrication conditions are extremely poor ($\Lambda \ll 1$); significant metal-to-metal contact occurs as the surface asperities of the contacting parts are higher than the oil film thickness. The variation of bearing life factors (product of $a_1 a_2 a_3$), against the operating temperature, is given in Fig. 9(c) for ball-and-roller bearings. As seen, life factors as high as 12 under ideal operating conditions dramatically drop to 0.81 under unfavorable operating conditions.

With the consideration of lubrication effects, reduction in bearing lives with increasing temperature becomes even more dramatic. This is shown in Fig. 10, where modified L_{10} lives of all three bearings are plotted against the operating temperature. As seen, the modified L_{10} life of CRB reduces from 95,000 to 284 h, as a combined result of negative operating clearances and poor lubrication conditions.

Clearance Optimization Study

In the preceding section, it is shown that the performance of the high-speed system is greatly affected by the operating clearance of the CRB, which is dependent on the bearing manufactured clearance, interference tightness, and the temperature distribution across the bearing. It turns out that the operating clearance of the CRB is not only critical for the individual performance of the bearing, but it influences the performance of other two bearings by affecting system deflections and load distribution among bearings. It is also observed that the thermal preloads induced on the CRB are more critical than those induced on the ball bearings since negative operating clearance for a CRB is never desired.

These observations highlight the necessity for an attentive selection of bearing manufactured clearance that will not only yield satisfactory results under ideal situations; rather, which makes the bearing perform well over a broader range of operating conditions. To achieve this, this section introduces a clearance optimization study for the CRB considering a broad range of operating conditions. Results of the study are presented in terms of operation condition maps that clearly point out the desired and undesired clearance zones for the CRB at different operating points.

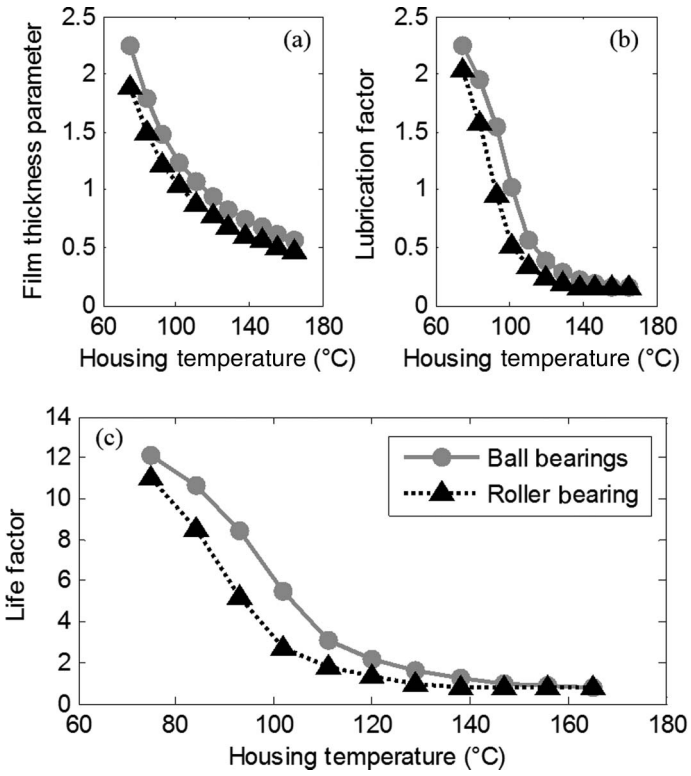

Fig. 9. Variation of (a) film thickness parameter, (b) lubrication factor, and (c) life factor for ball and roller bearings of the high-speed system with increasing temperature.

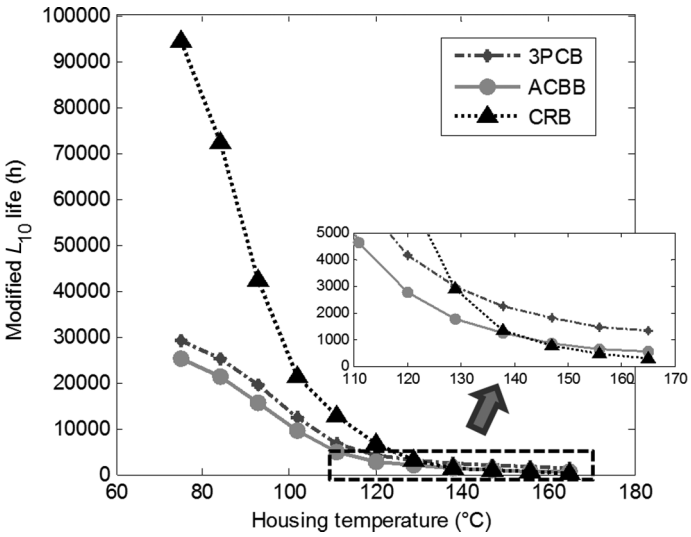

Fig. 10. Reduction in modified L_{10} life of system bearings with increasing operating temperature.

Cylindrical roller bearing

A full factorial optimization routine is run by varying the CRB manufactured clearance from 0 to 60 μm with 5 μm increments. For each of these data points, the mounted clearance is first calculated assuming a light interference fit of the outer ring to the liner. Then, for the 11 operating points (shown in Fig. 5), operating clearance of the CRB is calculated; this way a 143 element (11 $\times$ 13) operating clearance matrix is formed.

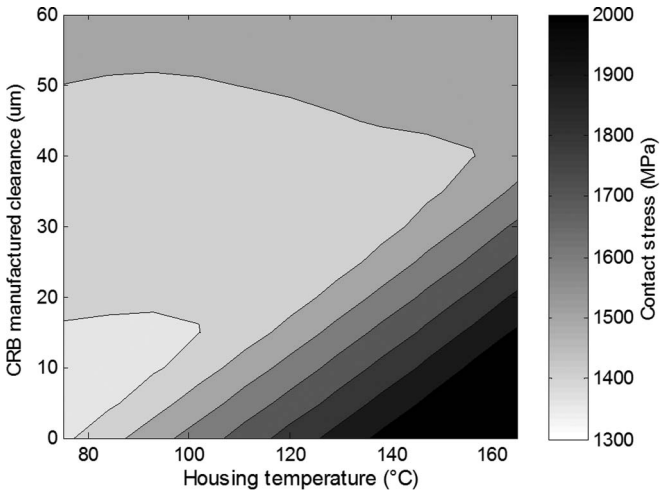

Fig. 11. Maximum contact stress map of CRB for different manufactured clearances and increasing operating temperature.

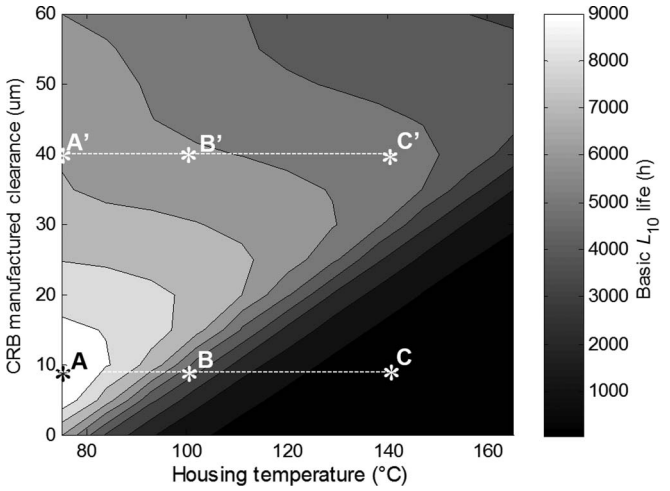

Fig. 12. Basic L_{10} life map of CRB for different manufactured clearances and increasing operating temperature.

At each of these points, maximum contact stresses on bearing raceways and basic L_{10} life of the bearings are calculated according to Ref. 15. Modified L_{10} lives of the bearings are also determined based on Eq. (15) by incorporating material, heat treatment, and lubrication effects.

Maximum contact stress, basic L_{10}, and modified L_{10} life maps for the CRB are presented in Figs. 11–13, respectively. In each of these plots, white and light gray areas represent the desired operating zones, whereas black and dark gray areas correspond to dangerous zones that should be avoided. Moderate gray tones represent the areas of transition from acceptable to unacceptable. For consistency, a reverse color scale is used in contact stress versus life plots.

Figure 11 illustrates the maximum contact stress map for the CRB for varying manufactured clearance and operating temperature. It is seen that a low manufactured clearance (about 10 μm) gives considerably low contact stresses under ideal operating temperatures, by distributing the bearing load to higher number of rolling elements. However, when the temperature exceeds a certain value, such low clearances are not favorable anymore, and bearing raceways are subjected to excessive contact stresses. A larger manufactured clearance such as 40 μm, on the other hand, gives acceptable contact stress levels for a broad range of operating temperatures. This indicates that selecting the normal clearance

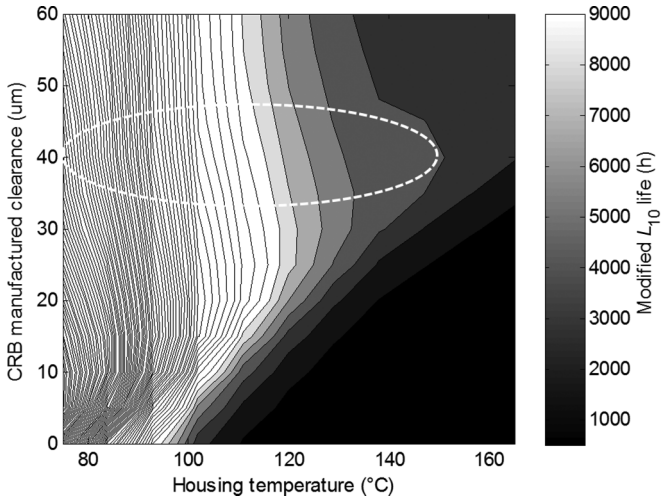

Fig. 13. Modified L_{10} life map of CRB for different manufactured clearances and increasing operating temperature.

class (CN), which correspond to an internal gap of 37.50 μm for a bearing of this size, is safer than selecting a tighter clearance class, such as C2 (17.50 μm), when a wider range of operation points is considered. Looser fits such as C3 (57.50 μm) and above are clearly not appropriate selections for this application as corresponding stress, and life results are poorer than those of the CN class in the entire operation range.

The significance of manufactured clearance on bearing performance can be more clearly observed on basic life results as shown in Fig. 12. Again, it is seen that an internal clearance as low as 10 μm gives the longest bearing life under ideal operating conditions ($T_h = 75°$C, denoted by point A). However, as soon as the temperature increases to 100°C (point B), basic life results immediately enter into the dark gray–black zone. For higher temperatures, such as $T_h = 140°$C, the bearing life is only 300 h (point C). Conversely, when a 40-μm manufactured clearance is selected, the bearing life remains in the light gray zone for all these three operation points (points A′, B′, and C′). Even at $T_h = 140°$C, basic L_{10} life is calculated as 5100 h (point C′).

With the consideration of material and lubrication effects, modified L_{10} life maps of high-speed bearings are similarly generated; Fig. 13 illustrates this map for the CRB. With the incorporation of the effects of special aerospace steels, bearing lives are greatly improved under ideal operating conditions (i.e., between $T_h = 75-100°$C). In this area. bearing lives reach as high as 100,000 h (practically infinite). Though to highlight the life range of interest and observe the transition zones, the maximum value of the color scale is limited to 9000 h for this figure. Here, it is seen that the curves representing equal-life areas become more vertical; meaning that the life become more dependent on the temperature, which partially conceals the effect of the clearance. This is because excellent (or conversely terrible) lubrication conditions essentially dictate the life of the bearing. One can notice that for $T_h > 140°$C, bearing life is always in the dark gray–black zone for all clearances. Yet, a manufactured clearance about 40 μm (order of CN class) gives the widest range of operating conditions that result in the acceptable L_{10} lives (this area is shown by the dashed ellipse in Fig. 13).

Effect of CRB clearance on ball bearings

It is earlier mentioned that the manufactured clearance of the CRB also affects the performance of ball bearings by influencing system deflections and load distributions. In this section, this cross-effect is explored.

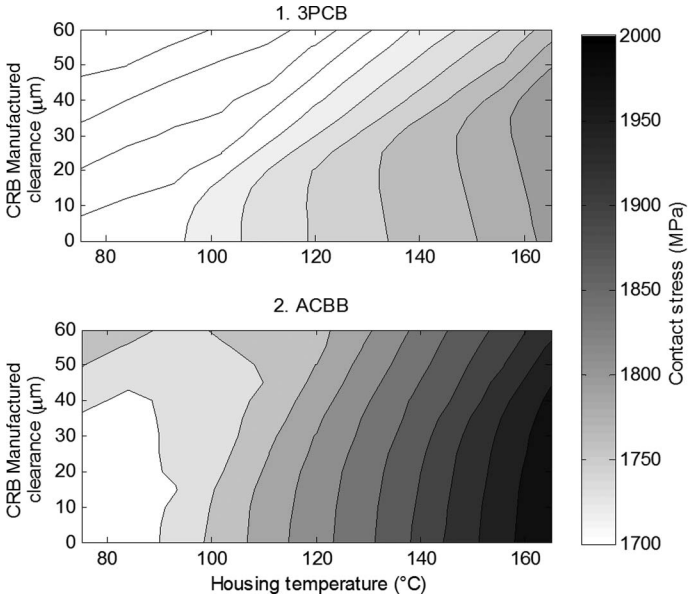

Fig. 14. Maximum contact stress map for ball bearings with respect to the manufactured clearance of the CRB and increasing operating temperature.

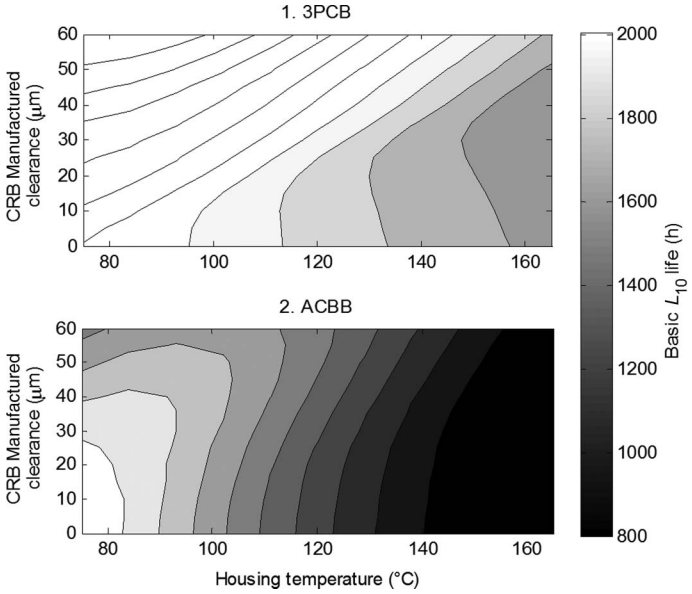

Fig. 15. Basic L_{10} life map for ball bearings with respect to the manufactured clearance of the CRB and increasing operating temperature.

Figures 14 and 15, respectively, display the variations of maximum contact stresses and basic L_{10} lives for two ball bearings. As a consequence of being closer to the gear mesh and being subjected to higher mesh loads, the stress and life results of ACBB (bearing 2) are more critical than 3 PCB (bearing 1). As the lines bounding equal-stress and equal-life areas become more horizontal, the influence of CRB clearance on ball bearings is more significant. For ACBB, this area corresponds to lower operating temperatures ($T_h < 90°$C). In this region, high clearance for the CRB reduces the life of ACBB due to increased moment load on ball bearings as expected. This trend tends to change above 90−95°C. Lower manufactured clearances at high temperatures cause CRB to

operate under extremely unfavorable conditions (i.e., negative operating clearance); this does not only affect the CRB itself, but the entire system including the duplex ball bearing. Therefore with increasing CRB clearance at high operating temperatures, some improvement in the ACBB life may be observed. When $T_h > 130^\circ$C, ACBB reaches unfavorable stress levels and lives due to reduced clearances and contact angle as a result of uneven thermal expansion of metal parts. In this dark gray–black zone, contact stresses and lives of the ACBB are less dependent on the CRB clearance. Stress and life results for 3 PCB are always within the acceptable range; thus, any performance improvement efforts should focus on bearings 2 and 3 for this high-speed bearing system. One should observe normal clearance class (37.50 μm), giving optimal results for a broad operation range.

Conclusions

Being the most critical components of the high-speed shaft, rolling element bearings face a number of operational challenges. Excessive friction and heat generation at the raceways may cause such bearings to reach undesired temperature levels when the cooling conditions are not ideal. It is found that the internal design of the bearings in microscale has a major influence on the performance of rolling bearings under unfavorable temperature conditions. Particularly, selection of an optimal internal clearance for the CRB is very critical to compensate for any thermally induced preloads that may dramatically reduce the bearing life.

To simulate this complex thermomechanical physics of the high-speed shaft, a comprehensive analytical model is proposed. The model describing the rolling element bearings as boundary conditions for the high-speed shaft is highly nonlinear due to the nature of the (Hertzian) contact between rolling element and raceways and the presence of internal clearances. The effects of interference mounting and uneven thermal expansion of bearing parts are included in this model. This allows the model to be effectively used to investigate the temperature elevations within the system.

A temperature elevation model, corresponding to a severe level of inadequate cooling, is then established to evaluate the performance of high-speed bearings with increasing temperature. It is seen that bearing contact stresses rise very rapidly with increasing temperature as a result of thermal preloads; consequently, dramatic reductions in high-speed bearing lives are seen particularly for the CRB. Although a tight internal clearance (C2 class) for this bearing gives an optimal load distribution under ideal conditions, it results in excessive contact stresses and significantly reduced bearing lives at higher temperatures. This indicates the requirement for the optimization of the roller bearing manufactured clearance considering a broad range of operating conditions.

By varying the manufactured clearance of the roller bearing and operating temperature, a full factorial optimization study is conducted. The optimization results confirm that although tight internal clearances give the finest results under normal operating temperatures, the range that they are effective is very narrow. As soon as the temperature of the system increases slightly, such low manufactured clearances become extremely dangerous for the bearing, causing increased friction, heat generation, and contact stresses due to negative operating clearances. The normal manufactured clearance (CN class), on the other hand, gives a smooth, satisfactory performance (in both component and system levels) over a broad operation range.

References

[1]Cope, G., "Model 427 Drive System," American Helicopter Society 55th Annual Forum Proceedings, Montreal, Quebec, Canada, May 25–27, 1999.

[2]Gasparini, G., Motta, N., and Straulino, G., "The 035 Main Gear Box: Strong, Light, Reliable and Silent Heart of the AW139 Helicopter," American Helicopter Society 63rd Annual Forum Proceedings, Virginia Beach, VA, May 1–3, 2007.

[3]Begin, L., Lopez, E., and Kerner, K., "Bearing Thermal Performance and Cage Slip Measurement for All-Steel and Ceramic Hybrid Compressor Thrust Bearings," American Helicopter Society 63rd Annual Forum Proceedings, Virginia Beach, VA, May 1–3, 2007.

[4]Gmirya, Y., Alulis, M., Palcic, P., and Leigh, L., "Design and Development of a Modern Transmission: Baseline Configuration of the CH-53K Drive System," American Helicopter Society 67th Annual Forum Proceedings, Virginia Beach, VA, May 3–5, 2011.

[5]Usuki, K., Akahori, H., Nakagawa, M., and Yamauchi, T., "Upgrade of Loss-of-Lubrication Operation Capability for EC145T2 (BK117 D-2) Main Gearbox," American Helicopter Society 69th Annual Forum Proceedings, Phoenix, AZ, May 21–23, 2013.

[6]Lin, C. H., Tu, J. F., and Kamman, J., "An Integrated Thermo-Mechanical-Dynamic Model to Characterize Motorized Machine Tool Spindles during Very High Speed Rotation," *International Journal of Machine Tools & Manufacture,* Vol. 43, 2003, pp. 1035–1050.

[7]Flouros, M., "Correlations for Heat Generation and Outer Ring Temperature of High Speed and Highly Loaded Ball Bearings in an Aero-Engine," *Aerospace Science and Technology,* Vol. 10, 2006, pp. 611–617.

[8]Jedrzejewski, J., Kowal, Z., Kwasny, W., and Modrzycki, W., "High-speed Precise Machine Tool Spindle Units Improving," *Journal of Materials Processing Technology,* Vol. 162–163, 2005, pp. 612–621.

[9]Jones, A. B., "A General Theory for Elastically Constrained Ball and Radial Roller Bearings under Arbitrary Load and Speed Conditions," *Journal of Basic Engineering*, Vol. 82, 1960, pp. 309–320.

[10]Lim, T. C., and Singh, R., "Vibration Transmission through Rolling Element Bearings, Part I: Bearing Stiffness Formulation," *Journal of Sound and Vibration*, Vol. 139, (2), 1990, pp. 179–199.

[11]Gunduz, A., and Singh, R., "Stiffness Matrix Formulation for Double Row Angular Contact Ball Bearings: Analytical Development and Validation," *Journal of Sound and Vibration*, Vol. 332, 2013, pp. 5898–5916.

[12]Coleman, T. F., and Li, Y., "On the Convergence of Interior-Reflective Newton Methods for Nonlinear Minimization Subject to Bounds," *Mathematical Programming*, Vol. 67, 1994, pp. 189–224.

[13]Harris, T. A., and Kotzalas, M. N., *Essential Concepts of Bearing Technology*, Taylor & Francis, Boca Raton, FL, 2006, Chap. 3.

[14]Harris, T. A., and Kotzalas, M. N., *Advanced Concepts of Bearing Technology*, Taylor & Francis, Boca Raton, FL, 2006, Chaps. 3 and 4.

[15]"Rolling Bearings—Methods for Calculating the Modified Reference Rating Life for Universally Loaded Bearings," ISO/TS 16281, International Standards Organization, 2008.

[16]Zaretsky, E. V., *STLE Life Factors for Rolling Bearings*, 2nd ed., STLE Publication SP-34.

[17]Rosado, L., Forster, H. F., Thompson, K. L., and Cooke, J. W., "Rolling Contact Fatigue Life and Spall Propagation of AISI M50, M50NiL, and AISI 52100, Part I: Experimental Results," *Tribology Transactions*, Vol. 53, 2010, pp. 29–41.